

# Graphene-substrate interaction on $6H\text{-SiC}(000\bar{1})$ : A scanning tunneling microscopy study

F. Hiebel, P. Mallet, F. Varchon, L. Magaud, and J-Y. Veuille  
*Institut Néel, CNRS-UJF, Boîte Postale 166, 38042 Grenoble, France*

(Received 10 July 2008; revised manuscript received 30 September 2008; published 28 October 2008)

The early stage of graphene formation on the  $6H\text{-SiC}(000\bar{1})$  surface is investigated by scanning tunneling microscopy. Islands made of a single graphitic plane form above regions of the substrate that show either a  $(2 \times 2)_C$  or a  $(3 \times 3)$  reconstruction. The orientations of the single-layer domains present a broad distribution of rotation angles with respect to the substrate. The atomic structures of the  $(3 \times 3)$  and  $(2 \times 2)_C$  substrate reconstructions are preserved under the first carbon layer. Low bias images reveal a graphitic structure, which indicates that the interaction between the first carbon plane and the SiC surface is comparatively much weaker on the C face than on the Si face of the substrate. The coupling is stronger on the  $(2 \times 2)_C$  surface reconstruction than on the  $(3 \times 3)$  one, where an almost ideal graphene structure is found close to the Fermi level.

DOI: [10.1103/PhysRevB.78.153412](https://doi.org/10.1103/PhysRevB.78.153412)

PACS number(s): 73.20.-r, 68.55.-a

The exceptional transport properties of graphene<sup>1-3</sup>—and especially the high carrier mobility—have stimulated an intense activity for developing graphene-based electronics. Among the various preparation techniques which have been proposed for this material,<sup>4-6</sup> the graphitization of polar surfaces of hexagonal SiC substrates appears as a promising way to produce large scale samples.<sup>4,7,8</sup> The objects produced in this way are known as few layer graphene (FLG). FLG samples can be obtained either on the  $(0001)$  (Si face) or  $(000\bar{1})$  (C face) of the substrate. So far physical (including transport) properties have mostly been studied on C face grown FLG samples.<sup>4,9,10</sup> Only one or two interface layers are believed to contribute to transport in these FLG films due to a charge transfer from the substrate.<sup>9</sup> It is therefore desirable to analyze in detail the structure of the interfacial layers to understand—and possibly to improve—the properties of the material. It turns out that the interaction with the environment is important also for the exfoliated graphene in view of recent results for suspended layers.<sup>11</sup> Therefore the characterization of the graphene-substrate interface is an important issue in general. This is best achieved using surface science techniques, and a lot of experimental and theoretical studies addressing this issue for Si face of the SiC substrate have been published recently.<sup>9,10,12-25</sup> These investigations have revealed (i) a strong interaction between the first graphitic C plane—the so-called buffer layer—and the SiC surface,<sup>15,21-23,25</sup> (ii) the formation of a genuine (electron doped) graphene layer on top of the interfacial structure,<sup>12-25</sup> (iii) the presence of a significant amount of disorder in the interface (buffer) layer below the first graphene plane,<sup>9,10,16-20</sup> and (iv) a possible interaction between the buffer layer and the upper graphene plane which might break the sublattice symmetry,<sup>21,24</sup> although this last point is debated. Surprisingly, only a few reports on the interface structure on the C face have been published. A strong interaction between the first graphitic layer and the substrate has been deduced from inverse photoemission<sup>26</sup> and x-ray reflectivity<sup>27</sup> experiments. Conversely, a photoemission study concludes that this interaction is quite weak.<sup>22</sup> In this Brief Report we present evidence for a rather weak coupling from scanning tunneling microscopy (STM) data taken in ultra-high vacuum at room temperature. We show moreover that

this interaction depends on the substrate reconstruction.

The samples were prepared as described previously.<sup>28</sup> The surface of the  $6H\text{-SiC}(000\bar{1})$  sample was first cleaned under ultrahigh vacuum to get the usual  $(3 \times 3)$  reconstruction.<sup>29,30</sup> Graphitization of the surface was performed by annealing at increasing power until a graphitic signal is detected by low energy electron diffraction (LEED). A typical diffraction pattern is shown in Fig. 1(a). The brightest spots correspond to the  $(3 \times 3)$  reconstruction of the substrate surface. Faint spots, indicated by the arrows, are due to the  $(2 \times 2)_C$  reconstruction of the substrate, which is known to coexist with the

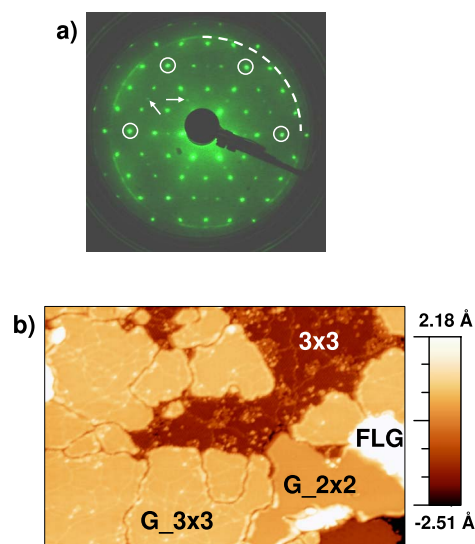


FIG. 1. (Color online) (a) LEED pattern of a  $6H\text{-SiC}(000\bar{1})$  sample at an early stage of graphitization. Electron beam energy: 78 eV. The circles indicate the  $(1 \times 1)$  SiC spots and the arrows point to faint SiC  $(2 \times 2)_C$  spots. The dashed (quarter) circle indicates the location of the graphene signal (spots or arcs). (b) STM image of the same sample, size:  $120 \times 80$  nm<sup>2</sup>, sample bias: +2.5 V. It shows a single substrate terrace, except for a step at the bottom right corner. The label  $3 \times 3$  indicates a bare substrate area with  $(3 \times 3)$  reconstruction,  $G_{3 \times 3}$  ( $G_{2 \times 2}$ ) a single graphitic layer covering a  $(3 \times 3)$  [ $(2 \times 2)_C$ ] reconstructed substrate region, and FLG a graphene multilayer area.

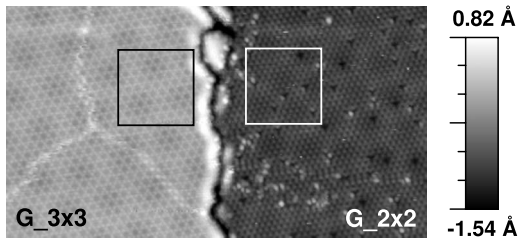


FIG. 2. Image of a region with a  $G_{3 \times 3}$  island (left side) and a  $G_{2 \times 2}$  island (right side). Size:  $40 \times 22 \text{ nm}^2$ ; sample bias:  $-2.0 \text{ V}$ . The  $(3 \times 3)$  and  $(2 \times 2)_C$  reconstructions of the substrate surface are visible. The large scale superstructures with periods of  $4.1 \text{ nm}$  (on  $G_{3 \times 3}$ ) or  $3.5 \text{ nm}$  (on  $G_{2 \times 2}$ ) are related to the presence of the graphitic overlayer.

$(3 \times 3)$  reconstruction upon annealing.<sup>22,30</sup> The graphite-related signal appears as spots [rotated by  $30^\circ$  with respect to  $\text{SiC}(1 \times 1)$ ] and arcs (rotated by  $15^\circ - 25^\circ$ ) arranged on an incomplete ring indicated by the dashed line. The LEED pattern thus reveals a significant distribution of rotation angles for the first graphene layer(s), but some preferential orientations exist, as shown by the strong intensity modulations along the ring. These results are in agreement with previous reports,<sup>8,10,22,26,31</sup> although the preferential orientations are different in detail, possibly due to differences in preparation procedures. An STM image of the same sample is presented in Fig. 1(b). It shows essentially a single  $\text{SiC}$  terrace, partially covered with islands of different heights. The lowest (base) level, labeled “ $3 \times 3$ ,” is the bare substrate surface with the usual  $(3 \times 3)$  reconstruction as judged from the similarity with high (positive and negative) bias STM images from the literature.<sup>29,30</sup> Islands with a typical lateral size of  $10\text{--}40 \text{ nm}$ , denoted as  $G_{2 \times 2}$  and  $G_{3 \times 3}$  in Fig. 1(b), form the second and third levels. They consist of one graphitic layer on top of the  $\text{SiC}(2 \times 2)_C$  or  $(3 \times 3)$  surface reconstruction as will be shown below. Their heights with respect to the bare  $(3 \times 3)$  surface are  $2.6$  and  $3.1 \text{ \AA}$ , which is indeed consistent with a single graphene plane on the substrate surface (these values are slightly bias and tip dependent). The structure labeled FLG is a multilayer graphene area, with height of  $9.0 \text{ \AA}$  above the bare  $(3 \times 3)$  plane.

In the following we concentrate on the  $G_{3 \times 3}$  and  $G_{2 \times 2}$  islands. Most of them present superlattices (SLs) with periods in the nanometer range. A typical example is shown in Fig. 2. The left part of the image is a  $G_{3 \times 3}$  island, which presents a SL with period  $4.1 \text{ nm}$  superimposed on a lattice with  $(3 \times 3)$  periodicity. One observes phase shifts of the SL on the bright wavy lines which are domain boundaries of the  $(3 \times 3)$  reconstruction, already reported in Ref. 30. The right part is a  $G_{2 \times 2}$  island. It presents a SL with a period of  $3.5 \text{ nm}$  and an underlying  $(2 \times 2)$  atomic structure. The corrugations of the SLs are bias dependent and have values ranging from  $0$  to  $0.25 \text{ \AA}$ . The periods of the SLs are related to the rotation of the graphenelike overlayers with respect to the  $\text{SiC}(1 \times 1)$  surface lattice, as for a moiré pattern. From atomic resolution images (see Fig. 3), the rotation angles measured in Fig. 2 are  $16^\circ \pm 2^\circ$  for the  $G_{3 \times 3}$  island and  $-22^\circ \pm 2^\circ$  for the  $G_{2 \times 2}$  island. Different periods and orientations of the SLs show up in large scale

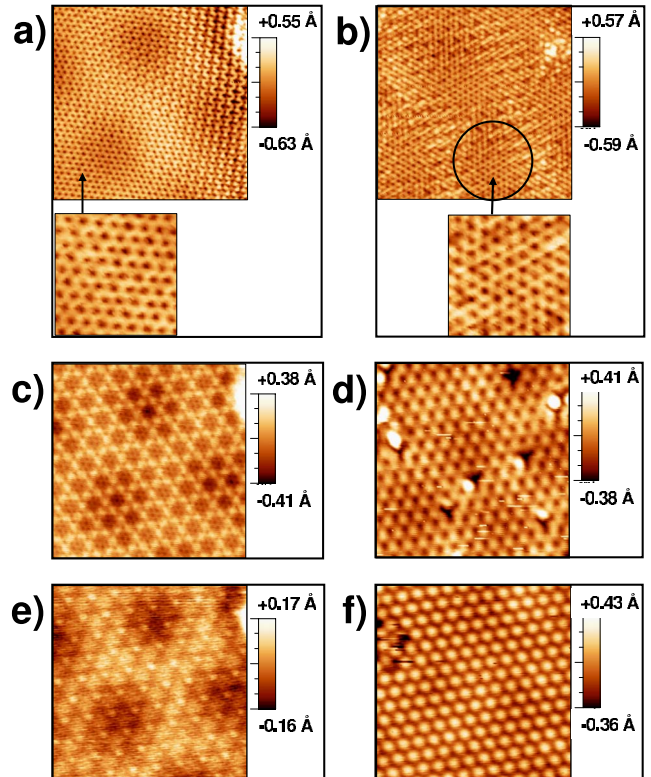


FIG. 3. (Color online) Images of the regions indicated by the boxes in Fig. 2 [(a), (c), and (e)] on the  $G_{3 \times 3}$  island and (b), (d), and (f) on the  $G_{2 \times 2}$  island. Size of the images:  $7.5 \times 7.5 \text{ nm}^2$ . [(a) and (b)] Low bias images (sample bias of  $-50 \text{ mV}$ ) of the  $G_{3 \times 3}$  and  $G_{2 \times 2}$  regions, respectively, showing a graphitic atomic structure. The insets are small scale images ( $2 \times 2 \text{ nm}^2$ ) zoomed in the areas indicated by the arrows to reveal the (local) honeycomb contrast. [(c) and (d)] High bias occupied state images (sample bias:  $-2.0 \text{ V}$ ) on the  $G_{3 \times 3}$  and  $G_{2 \times 2}$  islands, respectively. [(e) and (f)] High bias empty state images (sample bias:  $+2.5 \text{ V}$ ) on the  $G_{3 \times 3}$  and  $G_{2 \times 2}$  islands, respectively.

images for each type of islands,  $G_{2 \times 2}$  and  $G_{3 \times 3}$ . High resolution images taken on more than  $50$  islands reveal a broad distribution of rotation angles, ranging from  $9^\circ$  to  $30^\circ$  for  $G_{3 \times 3}$  islands and from  $6^\circ$  to  $30^\circ$  for  $G_{2 \times 2}$  ones (in absolute value), in agreement with the LEED data (for each island there is only one orientation of the graphitic layer). Therefore the “rotational disorder” observed on FLG obtained using similar preparation conditions<sup>28</sup> is already present in the first graphitic plane.

Small scale images of the zones indicated by square boxes in Fig. 2 are shown in Fig. 3. They are extracted from larger field images ( $20 \times 20 \text{ nm}^2$ ) covering the whole area, which insures that they are taken with the same tip on the  $G_{2 \times 2}$  and  $G_{3 \times 3}$  zones. We first discuss low bias images of  $G_{3 \times 3}$  and  $G_{2 \times 2}$  areas [Figs. 3(a) and 3(b)]. Both show atomic scale features with the lattice constant of graphene ( $0.246 \pm 0.006 \text{ nm}$ ) and—at least locally—the honeycomb pattern characteristic of the single layer<sup>16–20</sup> (see insets). This demonstrates that  $G_{2 \times 2}$  and  $G_{3 \times 3}$  islands are made of one graphitic layer as quoted previously. To gain insights into the underlying substrate structure, we take advantage from the fact that the graphene layer becomes “transparent”

at high bias.<sup>9,10,12,16–20</sup> High bias images of the  $G_{3\times 3}$  islands [Figs. 3(c) and 3(e)] show that the atomic scale features with the  $(3\times 3)$  periodicity consist of a single protrusion per unit cell at positive bias and a regular array of hexagonal holes at negative bias. This corresponds precisely to the observations made on the bare  $(3\times 3)$  reconstruction.<sup>29,30</sup> Therefore the initial surface structure of the substrate still exists under the graphene layer in the  $G_{3\times 3}$  island. Incidentally we notice that the interface seems to be well ordered at the atomic scale for the  $G_{3\times 3}$  phase at variance with the case of the Si face.<sup>9,10,16–20</sup> Figures 3(d) and 3(f) display high bias images of the  $G_{2\times 2}$  island. The  $2\times 2$  substrate atomic structure shows only one protrusion per unit cell at both polarities, in excellent agreement with published data for the bare  $(2\times 2)_C$  surface reconstruction.<sup>32</sup> Hence the graphitic overlayer also preserves the genuine  $(2\times 2)_C$  substrate structure.

From these observations, it appears that the first graphitic layer grows on top of the SiC substrate without causing a strong rearrangement of the surface structure. This is a major difference with respect to the Si face, where the growth of the first graphitic layer (the so-called “buffer layer”) induces a specific surface reconstruction [the  $6\sqrt{3}\times 6\sqrt{3}R(30^\circ)$ ], accompanied by the formation of chemical bonds between the substrate and the C overlayer.<sup>21–23</sup> As a consequence of this strong interaction on the Si face,  $C p_z$  (or  $\pi$ ) states are removed from the vicinity of the Fermi level for the buffer layer<sup>21,22</sup> and STM images do not reveal the graphene atomic lattice.<sup>18–20</sup> Conversely,  $C p_z$  (or  $\pi$ ) states are clearly seen at low bias for the first graphenelike plane on the C face, as shown in Fig. 3. An almost perfect honeycomb contrast is observed on the left part of the image for the  $G_{3\times 3}$  island [Fig. 3(a)]. Additionally, the right part of the image shows a  $\sqrt{3}\times\sqrt{3}R(30^\circ)$  superstructure due to intervalley electron scattering at the island boundary, which suggests that the Fermi surface of graphene is established at that stage.<sup>14,16</sup> All these observations indicate a very weak substrate-overlayer coupling for the  $G_{3\times 3}$  island, which essentially preserves the electronic structure of graphene close to the Fermi level  $E_F$ . The situation is different on the  $G_{2\times 2}$  island [Fig. 3(b)]. The honeycomb contrast is still observed in patches [circle in Fig. 3(b)] correlated with the SL period seen in Fig. 3(d). The atomic rows in adjacent patches are aligned but the graphene lattice looks somewhat perturbed in between. In particular, this perturbation gives rise to an array of dark triangles of atomic size, which look like “missing graphene atoms,” located on the edge of the patches in Fig. 3(b) and arranged with the  $(2\times 2)$  periodicity of the reconstructed SiC surface. This indicates a significant local interaction between the substrate and the graphene layer on the  $G_{2\times 2}$  island which alters the honeycomb contrast in STM. The observation of structures with the interatomic spacing of graphite in the perturbed areas [Fig. 3(b)] shows however that this coupling is insufficient to remove all the  $C p_z$  states from the vicinity of the Fermi level.

The previous observations have been corroborated on  $G_{2\times 2}$  and  $G_{3\times 3}$  islands with different orientations of the first graphitic layer. The  $(2\times 2)_C$  and  $(3\times 3)$  substrate reconstructions are always identified below the graphitic plane in high bias images. At low bias, we find an almost unperturbed graphene structure on the  $G_{3\times 3}$  islands, which confirms the weak substrate-overlayer coupling close to  $E_F$ . The interaction is apparently stronger for the  $G_{2\times 2}$  island, although a lattice with the periodicity of graphite (which eventually gives rise to graphenelike patches for rotation angles between  $14^\circ$  and  $22^\circ$ ) is still detected at low bias, which shows that  $C p_z$  states remain present close to  $E_F$ . At low energy, the graphene-substrate coupling thus appears to be much weaker on the C face than on the Si face, especially for the  $G_{3\times 3}$  phase. These findings are in agreement with a recent photoemission study,<sup>22</sup> which concludes from valence band and core-level spectra that the interaction between the first graphene layer and the substrate is small. In particular, they could observe the  $\pi$  band close to  $E_F$  for submonolayer graphene coverage. As also mentioned in Ref. 22, the distribution of rotation angles of the single-layer graphene flakes is also in favor of a weak interaction, which is unable to lock the orientation of the overlayer to the substrate. This weak-coupling picture is however at variance with the conclusions of previous x-ray reflectivity<sup>27</sup> and inverse photoemission<sup>26</sup> studies. In the former case, the difference might be ascribed to a different preparation procedure (a much higher temperature and non-UHV conditions were used in Ref. 27). In the latter case a strong interaction was derived from the absence of the  $\pi^*$  state approximately 4 eV above  $E_F$  for a graphene layer grown on the  $(2\times 2)_C$  substrate reconstruction.<sup>26</sup> The experiments were made in a specific direction,  $30^\circ$  off the SiC surface directions. Since we have analyzed several different orientations and since we concentrate on states close to  $E_F$ , our results are not necessarily in contradiction with the conclusions of Forbeaux *et al.*<sup>26</sup> for the  $G_{2\times 2}$  structure (and obviously not for the  $G_{3\times 3}$  structure not considered in Ref. 26).

To summarize, our STM analysis of the atomic and electronic structure of the first stages of graphitization of the  $6H\text{-SiC}(000\bar{1})$  surface indicates a rather weak interaction between the substrate and the first graphitic plane. This is especially true for the  $(3\times 3)$  surface reconstruction where the characteristic features of an almost unperturbed graphene structure are observed at low energy. The coupling seems to be stronger for the  $(2\times 2)_C$  surface reconstruction but, anyway, much smaller than the coupling of the first graphitic plane (buffer layer) on the Si face. This substrate and reconstruction dependent interaction may offer interesting possibilities for interface engineering.

This work was supported by the French ANR (“Graph-SiC” project) and by the Région Rhône-Alpes (program “Cible”). The authors thank J. Hass, E. Conrad, and C. Berger for fruitful discussions.



- <sup>1</sup>K. S. Novoselov, A. K. Geim, S. V. Morozov, D. Jiang, M. I. Katsnelson, I. V. Grigorieva, S. V. Dubonos, and A. A. Firsov, *Nature* (London) **438**, 197 (2005).
- <sup>2</sup>Yuanbo Zhang, Yan-Wen Tan, Horst L. Stormer, and Philip Kim, *Nature* (London) **438**, 201 (2005).
- <sup>3</sup>A. K. Geim and K. S. Novoselov, *Nature Mater.* **6**, 183 (2007).
- <sup>4</sup>C. Berger, Z. Song, T. Li, X. Li, A. Y. Ogbazghi, R. Feng, Z. Dai, A. N. Marchenkov, E. H. Conrad, P. N. First, and W. A. de Heer, *J. Phys. Chem. B* **108**, 19912 (2004).
- <sup>5</sup>K. S. Novoselov, D. Jiang, F. Schedin, T. J. Booth, V. V. Khotkevich, S. V. Morozov, and A. K. Geim, *Proc. Natl. Acad. Sci. U.S.A.* **102**, 10451 (2005).
- <sup>6</sup>Peter W. Sutter, Jan-Ingo Flege, and Eli A. Sutter, *Nature Mater.* **7**, 406 (2008).
- <sup>7</sup>I. Forbeaux, J.-M. Themlin, and J.-M. Debever, *Phys. Rev. B* **58**, 16396 (1998).
- <sup>8</sup>J. Hass, R. Feng, T. Li, Z. Zong, W. A. de Heer, P. N. First, E. H. Conrad, C. A. Jeffrey, and C. Berger, *Appl. Phys. Lett.* **89**, 143106 (2006).
- <sup>9</sup>C. Berger, Z. Song, X. Li, X. Wu, N. Brown, C. Naud, D. Mayou, T. Li, J. Hass, A. N. Marchenkov, E. H. Conrad, P. N. First, and W. A. de Heer, *Science* **312**, 1191 (2006).
- <sup>10</sup>W. A. de Heer, C. Berger, X. Wu, P. N. First, E. H. Conrad, X. Li, T. Li, M. Sprinkle, J. Hass, M. L. Sadowski, M. Potemski, and G. Martinez, *Solid State Commun.* **143**, 92 (2007).
- <sup>11</sup>K. I. Bolotin, K. J. Sikes, Z. Jiang, M. Klima, G. Fudenberg, J. Hone, P. Kim, and H. L. Stormer, *Solid State Commun.* **146**, 351 (2008).
- <sup>12</sup>A. Charrier, A. Coati, T. Argunova, F. Thibaudau, Y. Garreau, R. Pinchaux, I. Forbeaux, J.-M. Debever, M. Sauvage-Simkin, and J.-M. Themlin, *J. Appl. Phys.* **92**, 2479 (2002).
- <sup>13</sup>A. Bostwick, T. Ohta, T. Seyller, K. Horn, and E. Rotenberg, *Nat. Phys.* **3**, 36 (2007).
- <sup>14</sup>G. M. Rutter, J. N. Crain, N. P. Guisinger, T. Li, P. N. First, and J. A. Stroscio, *Science* **317**, 219 (2007).
- <sup>15</sup>F. Varchon, R. Feng, J. Hass, X. Li, B. N. Nguyen, C. Naud, P. Mallet, J.-Y. Veuillen, C. Berger, E. H. Conrad, and L. Magaud, *Phys. Rev. Lett.* **99**, 126805 (2007).
- <sup>16</sup>P. Mallet, F. Varchon, C. Naud, L. Magaud, C. Berger, and J. Y. Veuillen, *Phys. Rev. B* **76**, 041403(R) (2007).
- <sup>17</sup>V. W. Brar, Y. Zhang, Y. Yayon, T. Ohta, J. L. McChesney, A. Bostwick, E. Rotenberg, K. Horn, and M. F. Crommie, *Appl. Phys. Lett.* **91**, 122102 (2007).
- <sup>18</sup>G. M. Rutter, N. P. Guisinger, J. N. Crain, E. A. A. Jarvis, M. D. Stiles, T. Li, P. N. First, and J. A. Stroscio, *Phys. Rev. B* **76**, 235416 (2007).
- <sup>19</sup>C. Riedl, U. Starke, J. Bernhardt, M. Franke, and K. Heinz, *Phys. Rev. B* **76**, 245406 (2007).
- <sup>20</sup>P. Lauffer, K. V. Emtsev, R. Graupner, T. Seyller, L. Ley, S. A. Reshanov, and H. B. Weber, *Phys. Rev. B* **77**, 155426 (2008).
- <sup>21</sup>Seungchul Kim, Jisoon Ihm, Hyoung Joon Choi, and Young-Woo Son, *Phys. Rev. Lett.* **100**, 176802 (2008).
- <sup>22</sup>K. V. Emtsev, F. Speck, Th. Seyller, L. Ley, and J. D. Riley, *Phys. Rev. B* **77**, 155303 (2008).
- <sup>23</sup>F. Varchon, P. Mallet, J.-Y. Veuillen, and L. Magaud, *Phys. Rev. B* **77**, 235412 (2008).
- <sup>24</sup>S. Y. Zhou, G.-H. Gweon, A. V. Fedorov, P. N. First, W. A. de Heer, D.-H. Lee, F. Guinea, A. H. Castro Neto, and A. Lanzara, *Nature Mater.* **6**, 770 (2007).
- <sup>25</sup>A. Mattausch and O. Pankratov, *Phys. Rev. Lett.* **99**, 076802 (2007).
- <sup>26</sup>I. Forbeaux, J.-M. Themlin, and J.-M. Debever, *Surf. Sci.* **442**, 9 (1999).
- <sup>27</sup>J. Hass, R. Feng, J. E. Millan-Otoya, X. Li, M. Sprinkle, P. N. First, W. A. de Heer, E. H. Conrad, and C. Berger, *Phys. Rev. B* **75**, 214109 (2007).
- <sup>28</sup>F. Varchon, P. Mallet, L. Magaud, and J.-Y. Veuillen, *Phys. Rev. B* **77**, 165415 (2008).
- <sup>29</sup>H. E. Hoster, M. A. Kulakov, and B. Bullemer, *Surf. Sci.* **382**, L658 (1997).
- <sup>30</sup>J. Bernhardt, M. Nerding, U. Starke, and K. Heinz, *Mater. Sci. Eng., B* **61-62**, 207 (1999).
- <sup>31</sup>J. Hass, F. Varchon, J. E. Millan-Otoya, M. Sprinkle, N. Sharma, W. A. de Heer, C. Berger, P. N. First, L. Magaud, and E. H. Conrad, *Phys. Rev. Lett.* **100**, 125504 (2008).
- <sup>32</sup>A. Seubert, J. Bernhardt, M. Nerding, U. Starke, and K. Heinz, *Surf. Sci.* **454-456**, 45 (2000).